

# Superconductivity in CuAl<sub>2</sub>-type Co<sub>0.2</sub>Ni<sub>0.1</sub>Cu<sub>0.1</sub>Rh<sub>0.3</sub>Ir<sub>0.3</sub>Zr<sub>2</sub> with a high-entropy-alloy transition metal site

Yoshikazu Mizuguchi<sup>a</sup> and Tatsuma D. Matsuda<sup>a</sup>

<sup>a</sup>Department of Physics, Tokyo Metropolitan University, 1-1, Minami-osawa, Hachioji, 192-0397

## Abstract

Research on high-entropy-alloy (HEA) superconductors is one of the growing fields in material science. In this study, we have explored new HEA-type superconductors and discovered a CuAl<sub>2</sub>-type superconductor Co<sub>0.2</sub>Ni<sub>0.1</sub>Cu<sub>0.1</sub>Rh<sub>0.3</sub>Ir<sub>0.3</sub>Zr<sub>2</sub> with a HEA-type transition metal site. A superconducting transition was observed at 8.0 K in electrical resistivity, magnetization, and specific heat measurements. Bulk characteristics of the superconductivity were confirmed by the specific heat measurements. The discovery of superconductivity in HEA-type Co<sub>0.2</sub>Ni<sub>0.1</sub>Cu<sub>0.1</sub>Rh<sub>0.3</sub>Ir<sub>0.3</sub>Zr<sub>2</sub> will provide us with a new playground for exploration of new HEA-type superconductors and investigations on the relationship between local structures and superconductivity in HEA-type compounds.

**Keywords:** high-entropy-alloy; material design; new superconductor; CuAl<sub>2</sub>-type structure

**Impact statement:** We report on the material design, synthesis, and observation of a superconducting transition at 8.0 K in new high-entropy-alloy-type compound Co<sub>0.2</sub>Ni<sub>0.1</sub>Cu<sub>0.1</sub>Rh<sub>0.3</sub>Ir<sub>0.3</sub>Zr<sub>2</sub> with a CuAl<sub>2</sub>-type structure.

## 1. Introduction

Recently, high-entropy alloys (HEAs) [1,2], which are defined as alloys containing five or more elements with a concentration between 5 to 35at%, have been extensively studied in the fields of material science, engineering, chemistry, and physics. Alloys synthesized with the criterion results in high configurational mixing entropy ( $\Delta S_{\text{mix}}$ ), which is defined as  $\Delta S_{\text{mix}} = -R \sum_i c_i \ln c_i$ , where  $c_i$  and  $R$  are compositional ratio and the gas constant, respectively [2]. In a HEA, mixed (five or more) elements are sometimes distributed randomly, and mixing elements sometimes results in the formation of nano-scale phase separations [3,4]. Such unique structural characteristics of HEAs have fascinated researchers in the field of superconductivity as well because nano-scale structural and/or electronic disorders could be useful for improving critical current density in some cases [5-7]. Recently, exploration and investigation of HEA superconductors have been a hot topic since the discovery of the first HEA superconductor  $\text{Ta}_{34}\text{Nb}_{33}\text{Hf}_8\text{Zr}_{15}\text{Ti}_{11}$  with a transition temperature  $T_c = 7.3$  K in 2014 [8,9]. After the discovery, various HEA superconductors with a simple alloy-type structure (bcc and hcp structures) have been discovered [9-15]. Although the pairing mechanisms of the superconductivity in those HEA superconductors have been characterized as a conventional type, the field has been getting attention because HEA superconductors possess exotic characteristics. For example, electrical resistance measurements under extremely high pressures revealed that the superconductivity states in Ta–Nb–Hf–Zr–Ti are robust under pressures up to 190 GPa [16]. This fact suggests that the HEA states may be useful to maintain the essential crystal structure and electronic states for the emergence of superconductivity under extreme conditions. In addition, as mentioned above, the concept of HEA should be useful for the research on improving critical current density of superconductors for practical use. Therefore, we need to extend the concept of HEA to various compounds other than bcc and hcp metals to develop the field of HEA-type superconductors.

In 2018, Stolze et al. reported superconductivity in CsCl-type  $(\text{Sc,Zr,Nb,Ta})_{0.65}(\text{Rh,Pd})_{0.35}$  [17]. Since a CsCl-type structure is composed of two different crystallographic sites, the  $(\text{Sc,Zr,Nb,Ta})_{0.65}(\text{Rh,Pd})_{0.35}$  superconductor can be regarded as a *HEA-type compound*. Recently, we have reported the synthesis and superconducting properties of HEA-type layered superconductors [18,19]. In a  $\text{BiS}_2$ -based layered superconductor system ( $\text{REO}_{0.5}\text{F}_{0.5}\text{BiS}_2$ :  $\text{RE} = \text{La, Ce, Pr, Nd, Sm}$ ), an increase in  $\Delta S_{\text{mix}}$  improved superconducting properties due to the suppression of local structural disorder [20,21]. Single crystal growth and its superconducting properties of HEA-type  $\text{RE}(\text{O,F})\text{BiS}_2$  have also been reported; superconducting properties comparable to low-entropy systems were confirmed [22]. In a  $\text{RE123}$ -type cuprate system with  $\text{RE} = \text{Y, La, Pr, Nd, Sm, Eu, and Gd}$ , no degradation of  $T_c$  by an increase in  $\Delta S_{\text{mix}}$  was confirmed [19]. Therefore, the HEA effects in layered superconductors seem to be working positively or at least less-affecting. Recently, superconductivity in NaCl-type tellurides and related chalcogenides were reported [23-25]. For example, a HEA-type telluride  $\text{AgInSnPbBiTe}_5$  contains an HEA-type  $M$  site ( $M =$

Ag, In, Sn, Pb, Bi) and a Te site and shows superconductivity with  $T_c = 2.6$  K. In contrast to the cases of the layered systems, the superconducting properties of NaCl-type HEA tellurides are lower than those for low-entropy tellurides [24]. These results imply that the crystal structure type and its dimensionality are related to the effects of high-entropy-alloying to superconducting properties in compounds.

We have explored new HEA-type compound in this study. We have focused on the  $\text{CuAl}_2$ -type ( $I4/mcm$ ) structure because over 100 superconductors could be found in a superconductor database (SuperCon, NIMS database) [26]. Among them,  $\text{RhZr}_2$  has the highest  $T_c$  of 11.3 K [27]. Furthermore, as summarized in Table I,  $\text{TrZr}_2$  ( $\text{Tr} = \text{Co}, \text{Ni}, \text{Rh}, \text{Ir}$ ) compounds all show superconductivity with  $T_c = 5.5, 1.6, 11.3,$  and  $7.5$  K, respectively [27]. Although  $\text{FeZr}_2$  is a superconductor, its  $T_c$  is lower than 1 K [28,29]. In the case of  $\text{Tr} = \text{Cu}$ ,  $\text{CuZr}_2$  has a  $\text{CuZr}_2$ -type ( $I4/mmm$ ) structure, but partial substitution of Cu for the  $\text{CuAl}_2$ -type compounds is possible and positively affects on  $T_c$ . In  $\text{Co}_{1-x}\text{Cu}_x\text{Zr}_2$ , the  $T_c$ s for  $x = 0.05$  and  $0.1$  are higher than that for  $x = 0$  [30]. According to the  $T_c$  and the crystal structure of those  $\text{TrZr}_2$  compounds, we have designed a new possible HEA-type compound  $\text{Co}_{0.2}\text{Ni}_{0.1}\text{Cu}_{0.1}\text{Rh}_{0.3}\text{Ir}_{0.3}\text{Zr}_2$ , in which the composition at the  $\text{Tr}$  site meets the compositional criterion of HEA and achieves  $\Delta S_{\text{mix}} \sim 1.5R$  for the  $\text{Tr}$  site.

**Table 1. Crystal structure type, space group, and  $T_c$  of  $\text{TrZr}_2$  and related phases ( $\text{Tr} = \text{Co}, \text{Ni}, \text{Cu}, \text{Rh},$  and  $\text{Ir}$ ).**

Phase	Structural type	Space group	$T_c$ (K)	Reference ( $T_c$ )
$\text{CoZr}_2$	$\text{CuAl}_2$ -type	$I4/mcm$ (No. 140)	5.5	[27]
$\text{NiZr}_2$	$\text{CuAl}_2$ -type	$I4/mcm$ (No. 140)	1.6	[27]
$\text{RhZr}_2$	$\text{CuAl}_2$ -type	$I4/mcm$ (No. 140)	11.3	[27]
$\text{IrZr}_2$	$\text{CuAl}_2$ -type	$I4/mcm$ (No. 140)	7.5	[27]
$\text{FeZr}_2$	$\text{CuAl}_2$ -type	$I4/mcm$ (No. 140)	< 1 K	[28,29]
$\text{CuZr}_2$	$\text{CuZr}_2$ -type	$I4/mmm$ (No. 139)	-	-
$\text{Co}_{0.9}\text{Cu}_{0.1}\text{Zr}_2$	$\text{CuAl}_2$ -type	$I4/mcm$ (No. 140)	6.1	[30]
$\text{Co}_{0.2}\text{Ni}_{0.1}\text{Cu}_{0.1}\text{Rh}_{0.3}\text{Ir}_{0.3}\text{Zr}_2$	$\text{CuAl}_2$ -type	$I4/mcm$ (No. 140)	7.8	This work

## 2. Methods

A polycrystalline sample of  $\text{Co}_{0.2}\text{Ni}_{0.1}\text{Cu}_{0.1}\text{Rh}_{0.3}\text{Ir}_{0.3}\text{Zr}_2$  was synthesized by arc melting in Ar atmosphere. Powders of pure metals, Co (99%), Ni (99.9%), Cu (99.9%), Rh (99.9%), and Ir (99.9%), were mixed with a certain composition and pelletized. The metal pellet and a plate of pure Zr (99.2%) were used as starting materials for arc melting. The obtained sample was characterized by energy dispersive X-ray

fluorescence analysis on JSX-1000S (JEOL). The phase purity and the crystal structure were examined by X-ray diffraction (XRD) with Cu-K $\alpha$  radiation on Miniflex-600 (RIGAKU) equipped with a high-resolution semiconductor detector D/tex-Ultra. The obtained XRD pattern was refined by the Rietveld method using RIETAN-FP [31], and schematic images of the refined crystal structure were depicted using VESTA [32]. Magnetization was measured by a superconducting quantum interference device (SQUID) on MPMS-3 (Quantum Design). The temperature dependence of magnetization was measured both after zero-field cooling (ZFC) and field cooling (FC). The magnetic field dependence of magnetization was measured from -7 to 7 T. The temperature dependence of electrical resistivity under magnetic fields up to 3 T was measured by a four-terminal method with a DC current of 5 mA on a GM refrigerator system (AXIS). The temperature dependence of specific heat was measured by a relaxation method on PPMS (Quantum Design) under 0 and 9 T.

### 3. Results and discussion

Here, we report on the discovery of an HEA-type superconductor  $\text{Co}_{0.2}\text{Ni}_{0.1}\text{Cu}_{0.1}\text{Rh}_{0.3}\text{Ir}_{0.3}\text{Zr}_2$  with  $T_c = 8$  K, at which the onsets of superconducting transition were observed in the temperature dependences of magnetization, electrical resistivity, and specific heat. The sample obtained by arc melting was silver-coloured. The calculated sample-weight loss during the pelletizing and arc-melting processes was less than 1%. The measured composition of the sample was  $\text{Co}_{0.187}\text{Ni}_{0.097}\text{Cu}_{0.083}\text{Rh}_{0.328}\text{Ir}_{0.305}\text{Zr}_2$ , which was calculated by fixing the Zr amount as 2. Although slight deviation of the measured composition from the nominal starting composition was observed, the measured composition was close to the nominal value. Therefore, we call the sample  $\text{Co}_{0.2}\text{Ni}_{0.1}\text{Cu}_{0.1}\text{Rh}_{0.3}\text{Ir}_{0.3}\text{Zr}_2$  using the nominal value in this paper. Note that all the transition metal compositions are in a range of 5–35%, which meets one of the criteria of HEA. The calculated  $\Delta S_{\text{mix}}$  for the *Tr* site is  $1.47R$ .

Figure 1(a) shows the powder XRD pattern and the Rietveld refinement result. There is no clear indication of the presence of impurity phases. The refinement with a tetragonal  $\text{CuAl}_2$ -type ( $I4/mcm$ ) model resulted in a reliability factor of  $R_{\text{wp}} = 8.7\%$ . Refined lattice constants are  $a = 6.5006(2)$  Å and  $c = 5.5320(3)$  Å. The atomic coordinates are  $\text{Zr}(x, y, z) = (0.1639(3), 0.6659(3), 0)$  and  $T(x, y, z) = (0, 0, 0.25)$ . Schematic images of the refined crystal structure are shown in Figs. 1(b,c).

Figure 2(a) displays the temperature dependence of magnetization for  $\text{Co}_{0.2}\text{Ni}_{0.1}\text{Cu}_{0.1}\text{Rh}_{0.3}\text{Ir}_{0.3}\text{Zr}_2$ . Large diamagnetic signals, corresponding to the emergence of superconductivity, were observed below 7.8 K. Figure 2(b) shows the magnetic field dependence of magnetization ( $M$ - $H$ ) at 2.5 K. The data shows that superconducting currents are generated. The inset figure shows a  $M$ - $H$  plot at low fields, which confirms

that the lower critical field ( $\mu_0 H_{c1}$ ) is  $\sim 20$  mT. From those magnetization data, we confirmed that  $\text{Co}_{0.2}\text{Ni}_{0.1}\text{Cu}_{0.1}\text{Rh}_{0.3}\text{Ir}_{0.3}\text{Zr}_2$  is a typical type-II superconductor.

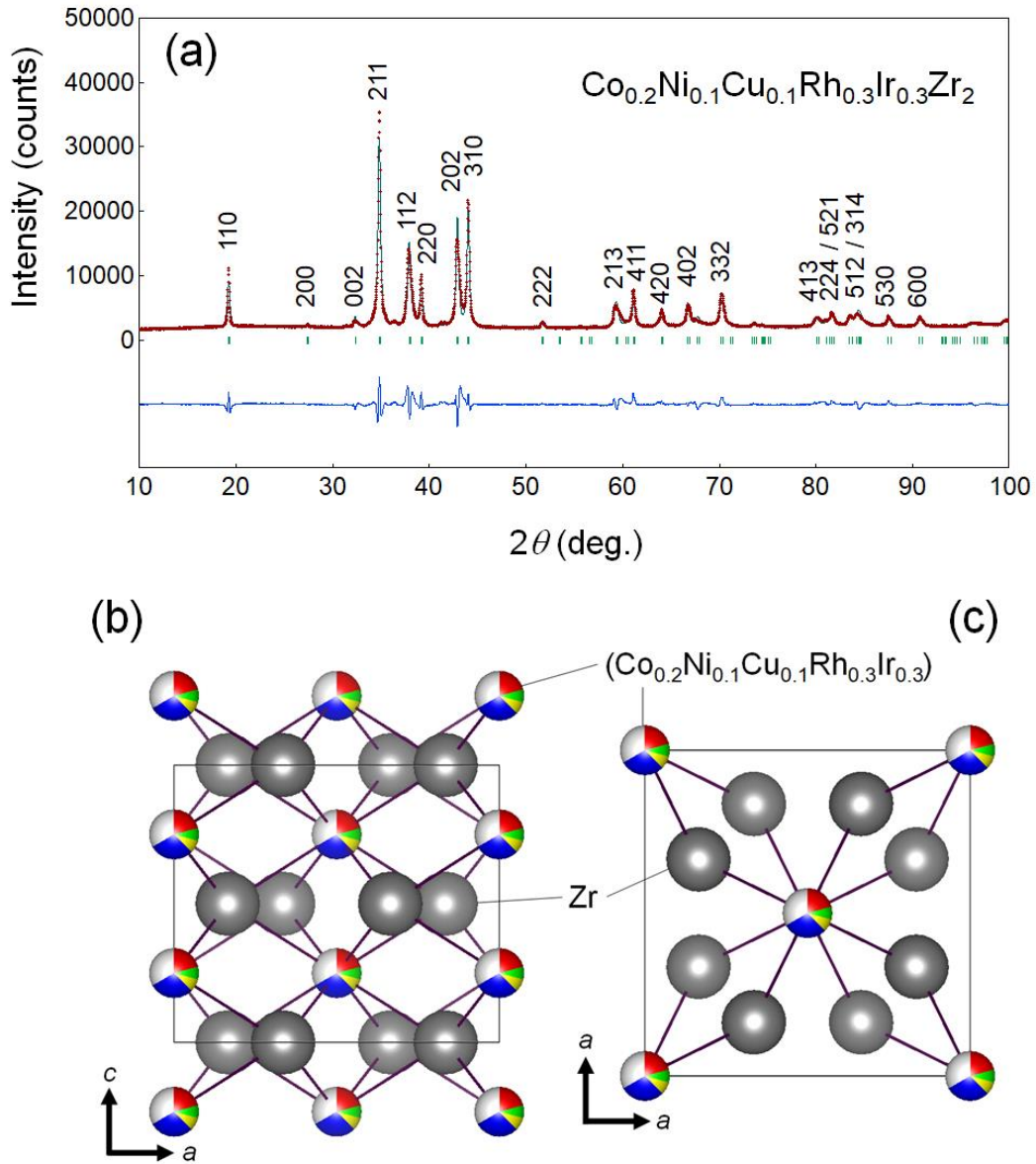


**Fig. 1. (a) XRD pattern and Rietveld fitting for  $\text{Co}_{0.2}\text{Ni}_{0.1}\text{Cu}_{0.1}\text{Rh}_{0.3}\text{Ir}_{0.3}\text{Zr}_2$ . The numbers in the figure are Miller indices. (b, c) Schematic images of crystal structure of  $\text{CuAl}_2$ -type  $\text{Co}_{0.2}\text{Ni}_{0.1}\text{Cu}_{0.1}\text{Rh}_{0.3}\text{Ir}_{0.3}\text{Zr}_2$ .**

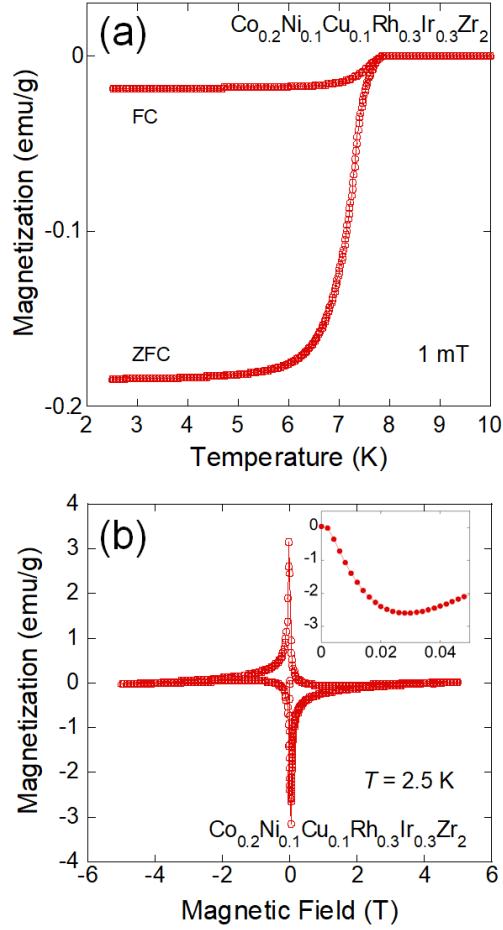
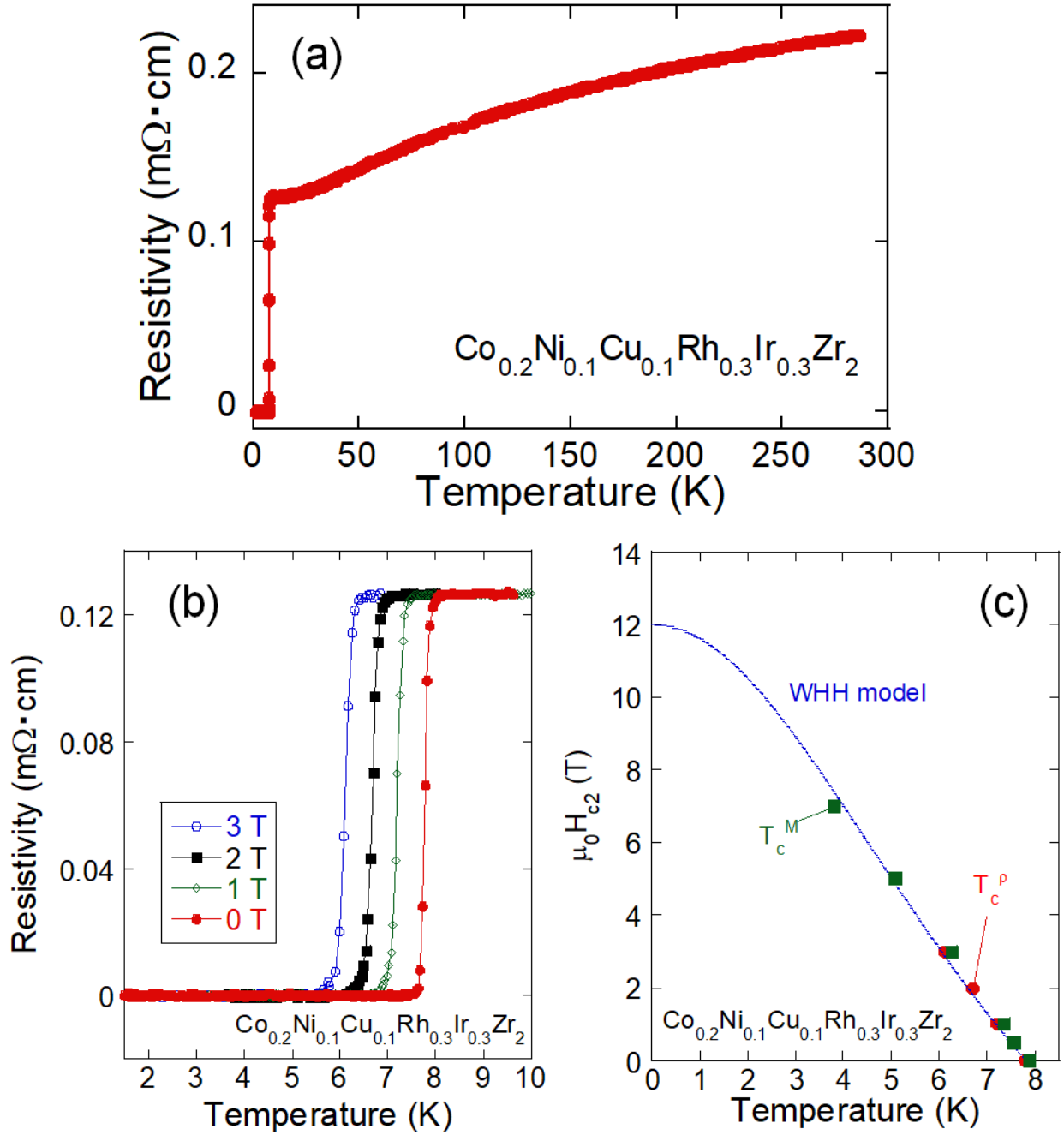


Fig. 2. (a) Temperature dependence of (ZFC and FC) magnetization for  $\text{Co}_{0.2}\text{Ni}_{0.1}\text{Cu}_{0.1}\text{Rh}_{0.3}\text{Ir}_{0.3}\text{Zr}_2$ . (b) Magnetic field dependence of magnetization for  $\text{Co}_{0.2}\text{Ni}_{0.1}\text{Cu}_{0.1}\text{Rh}_{0.3}\text{Ir}_{0.3}\text{Zr}_2$  taken at  $T = 2.5$  K. The inset shows low-field  $M$ - $H$  data.

Figure 3(a) shows the temperature dependence of electrical resistivity ( $\rho$ ) for  $\text{Co}_{0.2}\text{Ni}_{0.1}\text{Cu}_{0.1}\text{Rh}_{0.3}\text{Ir}_{0.3}\text{Zr}_2$ . Typical metallic behavior was observed, which is consistent to previous reports on  $\text{TrZr}_2$  compounds [27,33]. As shown in Fig. 3(b), the onset temperature ( $T_c^{\text{onset}}$ ) and the zero-resistivity temperature ( $T_c^{\text{zero}}$ ) are 8.0 and 7.5 K, respectively, at 0 T.  $T_c$  decreases with increasing magnetic field [Fig. 3(b)]. To estimate the upper critical field at 0 K [ $\mu_0 H_{c2}(0)$ ], the resistive midpoint  $T_c$  ( $T_c^{\rho}$ ) and magnetic  $T_c^M$  estimated from magnetization under various magnetic fields (see supplemental data) are plotted in a magnetic field-temperature phase diagram in Fig. 3(c). Using the WHH model (Werthamer-Helfand-Hohenberg model) [34], which is applicable for a dirty-limit type-II superconductor, the  $\mu_0 H_{c2}(0)$  was estimated as 12 T.



**Fig. 3.** (a) Temperature dependences of electrical resistivity for  $\text{Co}_{0.2}\text{Ni}_{0.1}\text{Cu}_{0.1}\text{Rh}_{0.3}\text{Ir}_{0.3}\text{Zr}_2$ . (b) Temperature dependences of resistivity for  $\text{Co}_{0.2}\text{Ni}_{0.1}\text{Cu}_{0.1}\text{Rh}_{0.3}\text{Ir}_{0.3}\text{Zr}_2$  under magnetic fields. (c) Magnetic field-temperature phase diagram for  $\text{Co}_{0.2}\text{Ni}_{0.1}\text{Cu}_{0.1}\text{Rh}_{0.3}\text{Ir}_{0.3}\text{Zr}_2$ .

To confirm the bulk nature of the observed superconductivity, specific heat was measured on a small piece (4.384 mg) of  $\text{Co}_{0.2}\text{Ni}_{0.1}\text{Cu}_{0.1}\text{Rh}_{0.3}\text{Ir}_{0.3}\text{Zr}_2$ . Figure 4(a) shows the temperature dependences of specific heat under 0 and 9 T. A clear jump was observed below 8.0 K under 0 T, but no superconducting

transition was observed under 9 T. Therefore, we used the data under 9 T to estimate the electronic specific heat coefficient ( $\gamma$ ) and the coefficient for lattice specific heat contribution ( $\beta$ ). The estimated  $\gamma$  and  $\beta$  are 20.7 mJ/mol·K<sup>2</sup> and 0.519 mJ/mol·K<sup>4</sup>. The Debye temperature ( $\theta_D$ ) was estimated as 224 K, which is close to that reported for a CoZr<sub>2</sub> single crystal [33]. To characterize the superconducting properties, the electronic contribution ( $C_{el}$ ) at 0 T, which was calculated by  $C_{el} = C - \beta T^3$ , is plotted in a form of  $C_{el}/T$  as a function of temperature in Fig. 4(b). The low temperature  $C_{el}/T$  data seems to approach zero at 0 K, suggesting bulk nature of the superconductivity. However, the superconducting transition seen from  $C_{el}$  is relatively broad as compared to a single crystal data for CoZr<sub>2</sub> [33]. The origin of the broad transition is not clear, but the present data is enough to confirm the emergence of bulk superconductivity in the examined sample. The superconducting jump in  $C_{el}$  ( $\Delta C_{el}$ ) estimated with  $T_c = 7.4$  K is  $1.12\gamma T_c$  (see supplemental data), which is a value consistent to the BCS model [35].

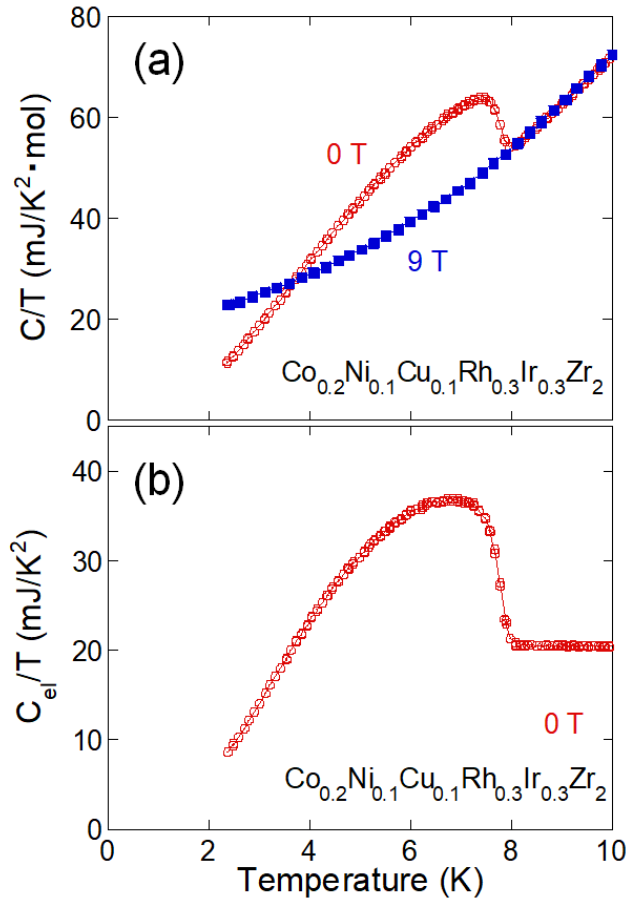


**Fig. 4. (a) Temperature dependence of  $C/T$  for  $\text{Co}_{0.2}\text{Ni}_{0.1}\text{Cu}_{0.1}\text{Rh}_{0.3}\text{Ir}_{0.3}\text{Zr}_2$  at 0 and 9 T. (b) Temperature dependence of electronic specific heat  $C_{el}/T$  at 0 T.**



To discuss about the effects of the HEA states in the  $Tr$  site of  $TrZr_2$  to superconducting properties, we compare the  $T_c$ s of pure  $TrZr_2$  and  $Co_{0.2}Ni_{0.1}Cu_{0.1}Rh_{0.3}Ir_{0.3}Zr_2$ . In known HEAs, properties or performance are sometimes close to the average for all the constituent metals and sometimes result in unexpectedly high or low values [17], which is so-called cocktail effects. In the case of  $T_c$  of  $Co_{0.2}Ni_{0.1}Cu_{0.1}Rh_{0.3}Ir_{0.3}Zr_2$ ,  $T_c = 8.0$  K seems to be close to the composition-weighted average value of  $T_c$ s for  $Tr = Co, Ni, Rh, \text{ and } Ir$ . Therefore, the cocktail effect-like improvement of  $T_c$  was not found in the present study. However, the present phase is just the first superconductor in the HEA-type  $TrZr_2$  systems, and we expect discoveries of various HEA-type  $TrZr_2$  superconductors and the improvement of superconducting properties in future works.

Here, we briefly describe future prospects of the HEA-type  $TrZr_2$  compounds. First, we expect that we can flexibly design various kinds of HEA-type  $TrZr_2$  according to the elemental and compositional design described in the introduction part of this paper. In a superconductor database [26],  $TrZr_2$ -type superconductors containing  $Tr = Sc, Fe, Co, Ni, Cu, Ga, Rh, Pd, Ta, \text{ and/or } Ir$  can be found. Therefore, the  $TrZr_2$  phases with a HEA-type  $Tr$  site will be useful for discussing the effects of long-range disorder, local phase separation, and/or modulation of local structure to superconducting properties. Furthermore, clarification of the HEA effects in superconductors will be important for the improvement of practical superconducting materials. Another possible merit of the HEA-type  $TrZr_2$  is the congruent melting character of the  $TrZr_2$  phases. As reported in Ref. 33, high quality single crystals can be obtained by simple melting. Therefore, the HEA-type  $TrZr_2$  phases will provide us with a platform to study the relationship between superconducting properties and HEA states using single crystals.

#### 4. Conclusion

We have reported the synthesis and superconducting properties of new HEA-type superconductor  $Co_{0.2}Ni_{0.1}Cu_{0.1}Rh_{0.3}Ir_{0.3}Zr_2$  with a HEA-type  $Tr$  site. The composition of  $Co_{0.2}Ni_{0.1}Cu_{0.1}Rh_{0.3}Ir_{0.3}Zr_2$  was designed based on information of the crystal structure (CuAl<sub>2</sub>-type) and  $T_c$  of the  $TrZr_2$  compounds from the NIMS database (SuperCon). A polycrystalline sample was prepared using pure metals by arc melting. A superconducting transition was observed at 8.0 K in magnetization, electrical resistivity, and specific heat measurements. From the magnetization and resistivity data under magnetic fields, the upper critical field  $\mu_0 H_{c2}(0)$  was estimated as 12 T. Specific heat data suggests that the superconductivity observed in the sample is bulk in nature. The estimated electronic specific heat coefficient and the Debye temperature are close to those reported on a  $CoZr_2$  single crystal. Although a cocktail effect, which is unexpected (non-average) improvements of the performance, was not observed on the  $T_c$  of  $Co_{0.2}Ni_{0.1}Cu_{0.1}Rh_{0.3}Ir_{0.3}Zr_2$ , the discovery of superconductivity in HEA-type  $TrZr_2$  should open a new playground for exploration of new

HEA-type superconductors and investigations on the relationship between local structures and superconductivity in HEA-type compounds.

#### **Declaration of interest statement**

We declare no competing interest.

#### **Declaration of interest statement**

Experimental data are available via reasonable requests to the corresponding author.

#### **Acknowledgements**

The authors thank R. Tsubota, N. Nakamura, A. Yamashita, and O. Miura for their assistance with the experiments. This work was partly supported by JSPS KAKENHI [Grant Number: 18KK0076] and the Advanced Research Program under the Human Resources Funds of Tokyo [Grant Number: H31-1].

#### **References**

- [1] Yeh J W, Chen S K, Lin S J, Gan J Y, Chin T S, Shun T T, Tsau C H, Chang S Y. Nanostructured High-Entropy Alloys with Multiple Principal Elements: Novel Alloy Design Concepts and Outcomes. *Adv. Eng. Mater.* 2004; 6: 299–303.
- [2] Tsai M H, Yeh J W. High-Entropy Alloys: A Critical Review. *Mater. Res. Lett.* 2014; 2: 107–123.
- [3] Feuerbacher M, Lienig T, Thomas C. A single-phase bcc high-entropy alloy in the refractory Zr-Nb-Ti-V-Hf system. *Scripta Materialia* 2018; 152: 40–43.
- [4] Manzoni A, Daoud H, Völkl R, Glatzel U, Wanderka N. Phase separation in equiatomic AlCoCrFeNi high-entropy alloy. *Ultramicroscopy* 2013; 132: 212–215.
- [5] Matsumoto K, Mele P. Artificial pinning center technology to enhance vortex pinning in YBCO coated conductors. *Supercond. Sci. Technol.* 2009; 23: 014001(1–12).
- [6] McElroy K, Lee J, Slezak J A, Lee D H, Eisaki H, Uchida S, Davis J C. Atomic-Scale Sources and Mechanism of Nanoscale Electronic Disorder in  $\text{Bi}_2\text{Sr}_2\text{CaCu}_2\text{O}_{8+\delta}$ . *Science* 2005; 309: 1048–1052.
- [7] Dou S X, Soltanian S, Horvat J, Wang X L, Zhou S H, Ionescu M, Liu H K. Enhancement of the critical current density and flux pinning of  $\text{MgB}_2$  superconductor by nanoparticle SiC doping. *Appl. Phys. Lett.* 2002; 81: 3419–3421.
- [8] Koželj P, Vrtnik S, Jelen A, Jazbec S, Jagličić Z, Maiti S, Feuerbacher M, Steurer W, Dolinšek J. Discovery of a Superconducting High-Entropy Alloy. *Phys. Rev. Lett.* 2014; 113: 107001(1–5).

- [9] Sun L, Cava R J. High-entropy alloy superconductors: Status, opportunities, and challenges. *Phys. Rev. Mater.* 2019; 3: 090301(1–10).
- [10] Marik S, Varghese M, Sajilesh K P, Singh D, Singh R P. Superconductivity in a new hexagonal high-entropy alloy. *Phys. Rev. Mater.* 2019; 3: 060602(1–6).
- [11] Vrtnik S, Kozelj P, Meden A, Maiti S, Steurer W, Feuerbacher M, Dolinsek J. Superconductivity in thermally annealed Ta-Nb-Hf-Zr-Ti high-entropy alloys. *J. Alloy Compound* 2017; 695: 3530–3540.
- [12] Stolze K, Cevallos F A, Kong T, Cava R J. High-entropy alloy superconductors on an  $\alpha$ -Mn lattice. *J. Mater. Chem. C* 2018; 6: 10441–10449.
- [13] Yuan Y, Wu Y, Luo H, Wang Z, Liang X, Yang Z, Wang H, Liu X, Lu Z. Superconducting  $\text{Ti}_{15}\text{Zr}_{15}\text{Nb}_{35}\text{Ta}_{35}$  High-Entropy Alloy With Intermediate Electron-Phonon Coupling. *Front. Mater.* 2018; 5: 72(1–6).
- [14] Ishizu N, Kitagawa J. New high-entropy alloy superconductor  $\text{Hf}_{21}\text{Nb}_{25}\text{Ti}_{15}\text{V}_{15}\text{Zr}_{24}$ . *Results in Phys.* 2019; 13: 102275(1–2).
- [15] von Rohr F O, Cava R J. Isoelectronic substitutions and aluminium alloying in the Ta-Nb-Hf-Zr-Ti high-entropy alloy superconductor. *Phys. Rev. Mater.* 2018; 2: 034801(1–7).
- [16] Guo J, Wang H, von Rohr F O, Wang Z, Cai S, Zhou Y, Yang K, Li A, Jiang S, Wu Q, Cava R J, Sun L, Robust zero resistance in a superconducting high-entropy alloy at pressures up to 190 GPa. *Proc. Natl. Acad. Sci. U.S.A.* 2017; 114: 13144–13147.
- [17] Stolze K, Tao J, von Rohr F O, Kong T, Cava R J. Sc–Zr–Nb–Rh–Pd and Sc–Zr–Nb–Ta–Rh–Pd High-Entropy Alloy Superconductors on a CsCl-Type Lattice. *Chem. Mater.* 2018; 30: 906–914.
- [18] Sogabe R, Goto Y, Mizuguchi Y. Superconductivity in  $\text{REO}_{0.5}\text{F}_{0.5}\text{BiS}_2$  with high-entropy-alloy-type blocking layers. *Appl. Phys. Express* 2018; 11: 053102(1–5).
- [19] Shukunami Y, Yamashita A, Goto Y, Mizuguchi Y. Synthesis of RE123 high-Tc superconductors with a high-entropy-alloy-type RE site. *Physica C* 2020; 572: 1353623(1–5).
- [20] Sogabe R, Goto Y, Abe T, Moriyoshi C, Kuroiwa Y, Miura A, Tadanaga K, Mizuguchi Y. Improvement of superconducting properties by high mixing entropy at blocking layers in  $\text{BiS}_2$ -based superconductor  $\text{REO}_{0.5}\text{F}_{0.5}\text{BiS}_2$ . *Solid State Commun.* 2019; 295: 43–49.
- [21] Mizuguchi Y, Hoshi K, Goto Y, Miura A, Tadanaga K, Moriyoshi C, Kuroiwa Y. Evolution of Anisotropic Displacement Parameters and Superconductivity with Chemical Pressure in  $\text{BiS}_2$ -Based  $\text{REO}_{0.5}\text{F}_{0.5}\text{BiS}_2$  (RE = La, Ce, Pr, and Nd). *J. Phys. Soc. Jpn.* 2018; 87: 023704(1–4).
- [22] Fujita Y, Kinami K, Hanada Y, Nagao M, Miura A, Hirai S, Maruyama Y, Watauchi S, Takano Y, Tanaka I. Growth and Characterization of  $\text{ROBiS}_2$  High-Entropy Superconducting Single Crystals. *ACS Omega* 2020; 5: 16819–16825.

- [23] Mizuguchi Y. Superconductivity in High-Entropy-Alloy Telluride  $\text{AgInSnPbBiTe}_5$ . *J. Phys. Soc. Jpn.* 2019; 88: 124708(1–5).
- [24] Kasem Md. R., Hoshi K, Jha R, Katsuno M, Yamashita A, Goto Y, Matsuda T D, Aoki Y, Mizuguchi Y. Superconducting properties of high-entropy-alloy tellurides  $\text{M-Te}$  (M: Ag, In, Cd, Sn, Sb, Pb, Bi) with a NaCl-type structure. *Appl. Phys. Express* 2020; 13: 033001(1–4).
- [25] Yamashita A, Jha R, Goto Y, Matsuda T D, Aoki Y, Mizuguchi Y. An efficient way of increasing the total entropy of mixing in high-entropy-alloy compounds: a case of NaCl-type  $(\text{Ag,In,Pb,Bi})\text{Te}_{1-x}\text{Se}_x$  ( $x = 0.0, 0.25, 0.5$ ) superconductors . *Dalton Trans.* 2020; 49: 9118–9122.
- [26] SuperCon, NIMS database; <https://supercon.nims.go.jp/supercon/>
- [27] Fisk Z, Viswanathan R, Webb G W. THE RELATION BETWEEN NORMAL STATE PROPERTIES AND  $T_c$  FOR SOME  $\text{Zr}_2\text{X}$  COMPOUNDS. *Solid State Commun.* 1974; 15: 1797–1799.
- [28] Matthias B T, Corenzwit E. Superconductivity of Zirconium Alloys. *Phys. Rev.* 1955; 100: 626–627.
- [29] Lefebvre J, Hilke M, Altounian Z. Superconductivity and short-range order in metallic glasses  $\text{Fe}_x\text{Ni}_{1-x}\text{Zr}_2$ . *Phys. Rev. B* 2009; 79: 184525(1–8).
- [30] Syu K J, Chen S C, Wu H H, Sung H H, Lee W H. Superconductivity in  $\text{Zr}_2(\text{Co}_{1-x}\text{Cu}_x)$ . *Physica C* 2013; 495: 10–14.
- [31] Izumi F, Momma K. Three-Dimensional Visualization in Powder Diffraction. *Solid State Phenom.* 2007; 130: 15–20.
- [32] Momma K, Izumi F. VESTA: a three - dimensional visualization system for electronic and structural analysis. *J. Appl. Crystallogr.* 2008; 41: 653–658.
- [33] Teruya A, Kakihana M, Takeuchi T, Aoki D, Honda F, Nakamura A, Haga Y, Matsubayashi K, Uwatoko Y, Harima H, Hedo M, Nakama T, Ōnuki Y. Superconducting and Fermi Surface Properties of Single Crystal  $\text{Zr}_2\text{Co}$ . *J. Phys. Soc. Jpn.* 2016; 85: 034706(1–10).
- [34] Werthamer N R, Helfand E, Hohenberg P C. Temperature and Purity Dependence of the Superconducting Critical Field,  $H_{c2}$ . III. Electron Spin and Spin-Orbit Effects. *Phys Rev.* 1966; 147: 295–302.
- [35] Bardeen J, Cooper L, Schrieffer J R. Theory of Superconductivity. *Phys. Rev.* 1957; 108: 1175–1204.

## Supplemental data

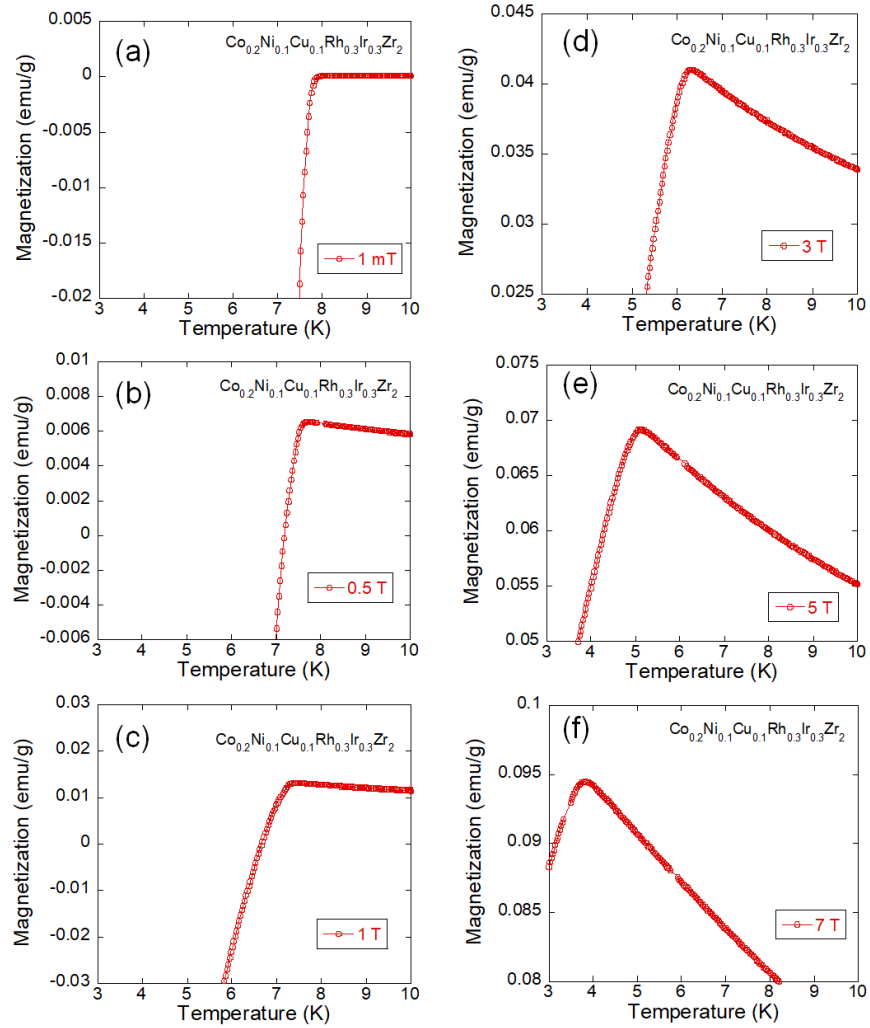


Fig. S1. Temperature dependences of magnetization for  $\text{Co}_{0.2}\text{Ni}_{0.1}\text{Cu}_{0.1}\text{Rh}_{0.3}\text{Ir}_{0.3}\text{Zr}_2$  under various magnetic fields.

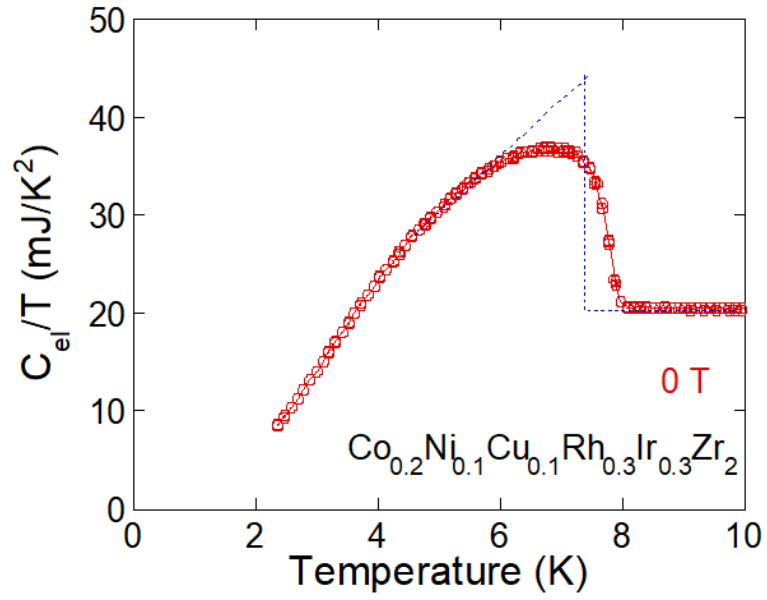


Fig. S2. Estimation of the electronic specific heat jump at  $T_c$  ( $=7.4$  K) for or  $\text{Co}_{0.2}\text{Ni}_{0.1}\text{Cu}_{0.1}\text{Rh}_{0.3}\text{Ir}_{0.3}\text{Zr}_2$  under 0 T.